

1 Original Article

2

3 **Geographically structured and temporally unstable growth responses of**  
4 ***Juniperus thurifera* to recent climate variability in the Iberian Peninsula**

5

6

7 **Lucía DeSoto<sup>1\*</sup>, Jesús Julio Camarero<sup>2</sup>, José Miguel Olano<sup>3</sup> and Vicente Rozas<sup>4</sup>**

8

9

10 <sup>1</sup> Centro de Ecología Funcional, Departamento de Ciências da Vida, Universidade de  
11 Coimbra, Apdo. 3046, 3001 - 456 Coimbra, Portugal.

12 <sup>2</sup>ARAID, Instituto Pirenaico de Ecología (CSIC), Avda. Montañana 1005, E-50080 Zaragoza,  
13 Spain;

14 <sup>3</sup> Área de Botánica, Departamento de Ciencias Agroforestales, EUI Agrarias, Universidad de  
15 Valladolid, Los Pajaritos s/n, E-42004 Soria, Spain;

16 <sup>4</sup> Misión Biológica de Galicia (MBG-CSIC), Apdo. 28, E-36080 Pontevedra, Spain.

17

18 \*Corresponding author: Lucía DeSoto

19 Centro de Ecología Funcional, Departamento de Ciências da Vida, Universidade de Coimbra,  
20 Apdo. 3046, 3001 - 456 Coimbra, Portugal.

21 Telephone no. +351 239 855219

22 Fax no. + 351 239 855211

23 E-mail: [luciadesoto@gmail.com](mailto:luciadesoto@gmail.com)

24

25 **Running head:** Geographical and climatic constraints of *Juniperus thurifera* growth

26 **Abstract**

27 Geographically structured tree-ring networks are needed to fully understand the spatio-  
28 temporal variability in climatic sensitiveness of trees and to study their future responses to  
29 global warming. We aim to identify the spatially-constrained structure of radial-growth  
30 patterns of the Spanish juniper (*Juniperus thurifera* L.) and to assess whether their climate-  
31 growth responses were unstable during the late twentieth century. Tree-ring width  
32 chronologies were built for 13 *J. thurifera* stands in Spain using dendrochronological methods  
33 and related to monthly climatic data. Sites were grouped according to their growth patterns  
34 using hierarchical cluster analysis. The relationships among geographical, climatic and stand  
35 features and their influence on radial growth were evaluated using redundancy analysis. The  
36 climate-growth relationships and their temporal stability were assessed using Pearson's and  
37 moving bootstrapped correlations, respectively. Stands formed three geographical groups  
38 according to their high-frequency growth variation: North West and Centre, North East, and  
39 South East. We found that *J. thurifera* radial-growth patterns depended on geographical and  
40 climatic factors, but not on the stand structure, and responded to a northwest-southeast  
41 gradient of decreasing rainfall and influence of Atlantic Westerlies and Mediterranean  
42 cyclonic activity. The positive response to June precipitation was unstable during the late 20th  
43 century and started earlier in populations from western mesic sites than in eastern xeric sites.  
44 This pattern may be related to either decreasing water availability in western than in eastern  
45 sites, or the resilience of *J. thurifera* growth from xeric sites in response to the increasing  
46 summer aridity.

47

48 **Keywords:** climate warming; dendrochronology; juniper; Mediterranean Basin; network;  
49 tree-ring.

## 50 **Introduction**

51 The current distribution areas of tree species in Europe are a consequence of historical  
52 processes such as glaciations or land-use changes and the capacity of each species to respond  
53 to environmental constraints such as climate (Svenning and Skov 2004). The role of these  
54 factors on determining the present range of several species has been evaluated (Davis and  
55 Shaw 2001) although detail studies about how past and current climatic constraints influence  
56 tree growth across the distribution area of selected European tree species are still needed.  
57 Such spatiotemporal assessment is required to forecast potential responses of tree growth to  
58 current climate warming throughout the species' distribution range. First, populations at the  
59 geographical margin of the range may show negative growth responses and decline processes  
60 (e.g. Macias et al. 2006). Second, nonlinear growth responses to the unprecedented rates of  
61 temperature rise and to the increase of climatic variability (e.g. more frequent and severe  
62 droughts) may also be expected and their effects may be more evident in harsh environments,  
63 such as marginal areas with pronounced water deficit (Andreu et al. 2007; Sarris et al. 2007).  
64 Finally, critical reviews of simulation models have emphasized that tree growth in central  
65 locations does not only respond to climate but also to other environmental factors (Loehle and  
66 LeBlanc 1996).

67 Nevertheless, few insights of growth patterns throughout most of the distribution area of  
68 tree species exist so as to compare the growth response to climate in central and marginal  
69 populations (Jump et al. 2006; Gaston 2009 and refs. therein). Such studies would provide a  
70 preliminary spatiotemporal analogy of growth responses to a changing climate because they  
71 would include central and marginal populations, potentially yielding divergent responses to  
72 contrasting climatic conditions. The current geographically diverse climates throughout the  
73 ranges of tree species might include climatic conditions similar to some of those predicted  
74 under the future warming.

75 Dendrochronology is an appropriate tool to describe tree-growth patterns and their  
76 dependence on climate at multiple spatial and temporal scales ranging from stands to whole  
77 distribution range and from years to centuries (e.g. Tardif et al. 2003). Common or divergent  
78 growth patterns among neighbouring or distant tree populations can reflect ecologically and  
79 climatically homogeneous territories (Cook et al. 2001; Piovesan et al. 2005; Di Filippo et al.  
80 2007) and can be used to detect geographical gradients for tree growth and forest productivity  
81 (Mäkinen et al. 2002; Carrer et al. 2007). Furthermore, networks of tree-ring chronologies  
82 have been increasingly used to detect geographical patterns in climate-growth relationships  
83 and even to describe the temporal stability of such relationships (Tardif et al. 2003; Carrer et  
84 al. 2007; Di Filippo et al. 2007). Nonetheless, the geographical and temporal variations of  
85 tree-ring growth across most of the distribution range of a tree species have been rarely  
86 assessed. Such spatiotemporal description would benefit from including climatically  
87 constraining sites (e.g. both water- and temperature-limited sites) which can provide a  
88 valuable analogue to the forecasted climate change conditions.

89 In the continental areas of the western Mediterranean Basin such as the Iberian Peninsula,  
90 summer drought and low winter temperatures are the main constraints of tree growth  
91 (Mitrakos 1980). Consequently, the growing season is split in two separated periods, spring  
92 and autumn, corresponding to the periods with enough water availability and mild  
93 temperatures (Camarero et al. 2010). In this area, several studies have reported a pronounced  
94 warming trend in the last decades, and a general decrease in precipitation in the  
95 Mediterranean margin of the Iberian Peninsula has been predicted (van Oldenborgh et al.  
96 2008). There is a great uncertainty on how such warming will affect tree growth in continental  
97 Mediterranean areas, where we can expect that rising temperatures may enhance growth in  
98 spring or autumn but increase water deficit in summer (Christensen et al. 2007). The observed  
99 growth declines and time-dependent climate-growth relationships in several Mediterranean

100 tree species have been attributed to increasingly drought-stress conditions induced by climate  
101 warming (Jump et al. 2006; Macias et al. 2006; Andreu et al. 2007; Carrer et al. 2007; Sarris  
102 et al. 2007; Linares et al. 2009). However, most of these studies were focused in reduced  
103 mountainous areas where the interaction between climatic and topographic factors causes  
104 complex spatiotemporal patterns of tree growth (Tardif et al. 2003; Leonelli et al. 2009).  
105 Hence, we need a detailed assessment of the impacts of climatic constraints on tree growth  
106 across most of the species distribution range but taking also into account the effects of  
107 topography on growth responses to climate.

108 The Iberian forests of Spanish juniper (*Juniperus thurifera* L.) provide the opportunity to  
109 solve the mentioned shortcomings since over 80 % of the world range of this tree, endemic to  
110 the western Mediterranean Basin, is located in Spain (Gauquelin et al. 1999). *Juniperus*  
111 *thurifera* is a long-lived evergreen species growing under continental and cold climatic  
112 conditions, dominating valuable ecosystems and forming unique landscapes (Fig. A1). Most  
113 extant populations are located at 300-3300 m elevation in Spain and Morocco, whereas relict  
114 populations exist in the French Alps and Pyrenees, Corsica and Algeria (Gauquelin et al.  
115 1999). These inland forests are affected by diverse climatic influences such as warmer and  
116 drier conditions in low-elevation sites towards the Mediterranean coast, and colder and more  
117 humid conditions towards the north-western Atlantic coast (Esteban-Parra et al. 1998;  
118 Rodríguez-Puebla et al. 1998). The comparative study of the sensitivity of this species to  
119 climatic patterns across geographical gradients in the Iberian Peninsula can provide a deeper  
120 understanding of the potential effects of climate change on inland Mediterranean ecosystems.

121 Thus, we can expect a geographic variation in the climatic response across the Iberian *J.*  
122 *thurifera* range, as a consequence to the west-east gradient of decreasing water availability in  
123 the Iberian Peninsula. We may also hypothesize that such growth response would be unstable  
124 through time being more marked during recent decades in response to warmer conditions and

125 lower water availability. To test whether the tree-growth sensitivity to climate is spatially  
126 structured and temporally stable over the last decades, we established a network of *J.*  
127 *thurifera* tree-ring chronologies in the Iberian Peninsula. Our specific aims were: (1) to  
128 characterize the spatiotemporal heterogeneity of radial-growth patterns across the Iberian  
129 distribution range of *J. thurifera*, (2) to identify the main geographical, topographical and  
130 climatic factors that determine this heterogeneity, and (3) to ascertain the temporal  
131 consistency of the limiting climatic factors that influence the growth of *J. thurifera* across its  
132 Iberian range.

133

## 134 **Material and methods**

### 135 **Study sites**

136 We sampled 13 *J. thurifera* stands located across its Iberian distribution range (38.5–43.5°  
137 N latitude and 0–6° W longitude), with elevations ranging from 350 to 1400 m (Table 1). *J.*  
138 *thurifera* was the dominant tree species in the stands and frequently coexisted with *Pinus* and  
139 *Quercus* species of diverse biogeographical origin (Table A1). Most *J. thurifera* forests in  
140 Spain are found typically in northern mountains (Fig. A1a; sites LA, LU), plateaus or canyons  
141 in calcareous ranges in the central Spanish Meseta (Fig. A1b; sites AR, BU, CA, CH, CI, OL,  
142 VE), and in semiarid or xeric eastern sites (Fig. A1c; sites RE, SA, VI). All study sites are  
143 subjected to a continental Mediterranean climate characterized by (1) summer drought, which  
144 increases from the North West to the South East in Spain (Fig. 1a), and (2) low winter  
145 temperatures with frequent frosts and snowfall throughout the continental Iberian distribution  
146 range of the species.

147

## 148 **Climatic data**

149 The climatic database used in this study corresponds to the TS 3.0 dataset produced by the  
150 Climate Research Unit (CRU 2008). This dataset is based on instrumental records from a  
151 network of meteorological stations over the global land surface which have been subjected to  
152 homogeneity tests and relative adjustments, and finally gridded onto a 0.5° network (Mitchell  
153 and Jones 2005). We downloaded monthly mean temperature (T) and total precipitation (P)  
154 data for the studied period using the Climate Explorer of the Royal Netherlands  
155 Meteorological Institute (<http://climexp.knmi.nl>).

156 Mean annual temperature ranged from 9.2 to 14.9 °C among study sites. January was the  
157 coldest month (mean minimum temperatures ranging from -3.4 to 2.2 °C) and July the  
158 warmest (mean maximum temperatures ranging from 23.7 to 33.0 °C). Mean annual  
159 precipitation was highly variable among study sites, ranging from 435 to 824 mm. May was  
160 the wettest month (45.0 – 79.2 mm) and July the driest one (7.1 – 37.7 mm), and water deficit  
161 occurred from June to September in most of the sites.

162

## 163 **Field sampling and dendrochronological methods**

164 We randomly selected 20 dominant mature trees without external signs of bole dieback in  
165 each stand. Diameter at breast height (DBH) and total height were measured in the main stem  
166 of each sampled tree. Two cores per tree were taken from opposite sides of the stem at 1.3 m  
167 above ground using an increment borer. At the Cabrejas site, the samples were stem disks  
168 from 23 mature trees taken at 1.3 m above ground (Rozas et al. 2009).

169 Wood samples were processed using standard dendrochronological procedures (Stokes and  
170 Smiley 1996). Cores and disks were dried, mechanically surfaced and then manually polished  
171 with a series of successively finer grades of sandpaper until the xylem cellular structure was  
172 clearly visible. After visual cross-dating, tree-ring widths were measured to the nearest 0.001

173 mm using a sliding-stage micrometer (Velmex Inc., Bloomfield, NY, US) interfaced with a  
174 computer. The individual tree-ring series were statistically compared with a site master  
175 chronology using the COFECHA program and checked for dating accuracy (Holmes 1983;  
176 Grissino-Mayer 2001). All series with potential errors were corrected when possible,  
177 including those containing missing or false rings, or discarded.

178 A site chronology was calculated from those ring-width series correctly synchronised  
179 within each site. Tree-ring width series were standardised with the ARSTAN program by  
180 using a two-step procedure (Cook and Holmes 1996). The series were first fit to a negative  
181 exponential function, and then to a cubic smoothing spline with a 50% frequency response of  
182 64 years, which was flexible enough to reduce the non-climatic variance by preserving high-  
183 frequency climatic information (Cook and Peters 1981). The obtained indices were averaged  
184 on a year-by-year basis using a biweight robust mean, and the mean series subjected to  
185 autoregressive modelling to obtain residual site chronologies of prewhitened growth indices  
186 (see Fig. 2). Several descriptive statistics were calculated for the common interval 1951-2002  
187 (Cook and Kairiukstis 1990; Fritts 1976) from the raw tree-ring widths (MW, SD and AC),  
188 and the residual site chronologies ( $ms_x$ ,  $r_{bt}$ , EPS, E1 and SNR). MW and SD are mean tree-  
189 ring width and their standard deviation, AC is the first-order autocorrelation, a measure of the  
190 year-to-year growth similarity. Mean sensitivity ( $ms_x$ ) is a measure of the year-to-year  
191 variability in width of consecutive tree rings, mean between-trees correlation ( $r_{bt}$ ) is a measure  
192 of the similarity in growth among trees, expressed population signal (EPS) is a measure of the  
193 statistical quality of the mean site chronology as compared with a perfect infinitely replicated  
194 chronology, percentage of variance explained by the first principal component (E1) is an  
195 estimate of the common variability in growth among all trees at each site, and signal-to-noise  
196 ratio (SNR) is a measure of the strength of the common high-frequency signal in the ring-



197 width indices of trees from the same site. The period with at least five trees in all site  
198 chronologies was regarded as the statistically reliable common period.

199

### 200 **Characterization of growth heterogeneity**

201 A hierarchical cluster analysis (HCA) was performed using the euclidean distances matrix  
202 between residual chronologies and based on the Minimum Evolution algorithm of Desper and  
203 Gascuel (2002) which fits the dendrogram to the data and determines the branch lengths  
204 (distances) by using unweighted least square methods. Therefore, least squares dendrograms  
205 were obtained for different topologies and then the topology of shortest total lengths among  
206 the sites was selected. The obtained clusters of residual chronologies were considered as  
207 homogeneous groups with similar high-frequency growth variation and validated by the  
208 bootstrap technique. We calculated the proportion of bootstrapped clusterings that support the  
209 groupings displayed in HCA analysis and stated them for each dendrogram node. HCA was  
210 performed with the *ape* package (Paradis et al. 2004) in the R environment (R Development  
211 Core Team 2010).

212

### 213 **Geographical determinants of tree-growth variability**

214 Distance-dependent relationships among site chronologies were assessed comparing their  
215 common growth variability, computed as the Pearson's correlations between all the site  
216 chronologies for the common period 1951-2002, as a function of the distance for all site pairs  
217 (teleconnection), calculated from the sites latitudes and longitudes (Carrer et al. 2010). To  
218 summarize the relationships among site chronologies a principal component analysis (PCA)  
219 was performed on a correlation matrix calculated among the chronologies considering the  
220 common period. The first two components of the PCA (PC1, PC2) were selected because they  
221 had eigenvalues greater than one (Garfin 1998). Lastly, linear or quadratic regressions

222 between stand characteristics (latitude, longitude, elevation) and statistics (MW, SD, AC,  $ms_x$ ,  
223  $r_{bt}$ , EPS, SNR, PC1 and PC2 of the network) were performed to recognise the geographical  
224 dependency of growth patterns.

225

### 226 **Growth-variation partitioning among geographical, climatic and stand variables**

227 The relative importance of geographical, climatic and stand features in determining the  
228 high-frequency variation of radial growth was evaluated via constrained ordinations (ter  
229 Braak 1986). Since the expected gradient was short, we performed a Redundancy Analysis  
230 (RDA) on the correlation matrix calculated among residual chronologies matrix. RDA  
231 searches those linear combinations of environmental factors (geographical, climatic and stand  
232 features) that are correlated to linear combinations of responses variables, in this case site  
233 residual chronologies (Legendre and Legendre 1998). We used three distinct environmental  
234 constraining matrices corresponding to three variance components to carry out RDAs: (a) a  
235 geographical matrix including elevation, longitude, latitude and the interaction term  
236 “longitude  $\times$  latitude”; (b) a climatic matrix including seasonal precipitations, Continentality  
237 Index (Gorczynski 1922), Mediterraneity Index (Rivas-Martínez and Rivas-Sáenz 2009),  
238 Aridity Index (De Martonne 1925) and annual average temperature; and (c) a stand-features  
239 matrix comprising mean tree age, DBH and height.

240 The total variation explained (TVE) by each environmental matrix was calculated as the  
241 sum of all canonical axes obtained using each of these matrices as a constraining data matrix  
242 (Borcard et al. 1992). The significance of the relationship was assessed using a Monte Carlo  
243 permutation test based on 999 randomizations. The sum of all canonical eigenvalues  
244 corresponded to the  $F$ -ratio statistic (ter Braak 1988), and it was considered significant when  
245  $P < 0.05$ . A forward stepwise procedure was carried out to select a reduced RDA model  
246 including only significant environmental variables for each environmental matrix. The

247 improvement of the reduced model with each new selected variable was determined by a  
248 Monte Carlo permutation test with 999 randomizations. Variance partitioning was performed  
249 to evaluate the relative importance of each component by adjusting the variability of the other  
250 components considered as covariables (Borcard et al. 1992). In this procedure, called partial  
251 RDA (pRDA), we calculated the fraction of growth variance explained independently by each  
252 environmental component. These analyses were done using Canoco v4.51 program for  
253 Windows (ter Braak and Šmilauer 1997; CANOCO Biometris, Wageningen, The  
254 Netherlands).

255

### 256 **Spatiotemporal variation of climate-growth relationships**

257 The climate-growth relationships were analysed at the regional level based on the  
258 composite chronologies corresponding to the geographical groups previously identified with  
259 HCA. The composite chronologies were computed averaging the site series of the same  
260 cluster (Carrer et al. 2007). To obtain climatic data for each regional group of chronologies,  
261 we used the MET routine in the Dendrochronology Program Library package (Holmes 1994).  
262 The mean temperature and precipitation data for each regional group were calculated as the  
263 average of the gridded temperature and precipitation data from all sites included in that group.

264 A temporal window of 13 months was selected to identify limiting climatic factors from  
265 September of the previous year ( $t-1$ ) to September of the year of tree-ring formation ( $t$ ).  
266 Pearson's correlations and bootstrapped response functions between growth indices and the  
267 climatic variables were calculated for the period 1951-2002 with the PRECON v5.17 program  
268 (Fritts et al. 1991). Bootstrapped moving correlations between these climatic variables and the  
269 composite regional chronologies were calculated considering 25-year intervals for the period  
270 1930-2006 using the Dendroclim2002 program (Biondi and Waikul 2004).

271

272

273 **Results**

274

275 **Geographical structure of tree growth variation**

276 Tree size showed high variability among sites, with mean DBH ranging between 13.9 and  
277 60.9 cm and mean height between 5.0 and 8.3 m (Table 1). Mean tree age varied from 50 to  
278 154 years. Tree-ring width ranged from 0.56 to 1.27 mm (Table 2), and differed significantly  
279 among sites (Kruskal-Wallis test:  $\chi^2_{12} = 301.2$ ;  $P < 0.001$ ) (Fig. 3a).

280 The first (PC1) and second (PC2) principal components of the entire *J. thurifera* network  
281 explained 43.57% and 10.65% of the growth variance, respectively, indicating a common  
282 signal at broad scales among all chronologies. No clear relationships between chronology  
283 statistics and geographical descriptors were evident, with the exceptions of PC2 loadings of  
284 residual chronologies that showed an inverse relationship with longitude (Fig. 3b), and mean  
285 sensitivities which increased with decreasing site elevation (Fig. 3c). The correlation between  
286 trees within each site ranged from 0.37 to 0.54, whereas the variance explained by the first  
287 eigenvector ranged from 34.5 to 58.8 % (Table 2). EPS varied from 0.84 to 0.94 confirming  
288 that the amount of local year-to-year growth variation shared by co-occurring trees was  
289 consistently high. Finally, the correlation among site chronologies decreased linearly as  
290 distance increased showing significant site-to-site correlations up to approximately 300 km  
291 (Fig. 3d).

292 Three groups with a consistent geographic pattern were established based on the HCA  
293 (Fig. 1b). Most of the bootstrapped cluster values within the groups highly supported the  
294 reliability of the clustering. The group of stands located in North West and Central Spain (40–  
295 43° N, 2.5–6.0° W; hereafter NW-C group) included six sites (LU, LA, AR, SI, CA and BU)

296 and 150 tree-ring series, and the first two principal components of this group explained 72 %  
297 of the total growth variance. A second group comprised four sites (CI, CH, RE and SA) in  
298 North East Spain (41–42° N, 0.0–2.5° W; hereafter NE group) and 94 tree-ring series, and its  
299 first two principal components explained 77 % of the growth variability. Finally, the last  
300 group included three sites (OL, VE and VI) from South East Spain (38.5–40.5° N, 0.5–3.0°  
301 W; hereafter SE group) and 71 tree-ring series, and its first two principal components  
302 explained 91 % of the common growth variance.

303

### 304 **Geographical and climatic constraints of tree growth**

305 The geographical and climatic components explained significant fractions of the total high-  
306 frequency variation of tree growth, whereas the stand-structure component did not  
307 significantly influence growth patterns (Table 3). The reduced RDA model of the  
308 geographical component included elevation and latitude as significant factors, and accounted  
309 for 30.5 % of the growth variance. The reduced model of climate included the Mediterraneanity  
310 Index and annual mean temperature, and accounted for 31.7 % of the variance. TVE  
311 explained by geographical and climatic data sets together was 49.4 % ( $F_{\text{ratio}} = 1.95$ ,  $P =$   
312  $0.001$ ), with an important fraction of shared variation (12.9 %). In fact, their separate effects  
313 on tree growth were only marginally significant (pRDA of climatic variables with  
314 geographical factors as covariates:  $F_{\text{ratio}} = 1.50$ ,  $P = 0.063$ ; pRDA of geographical factors with  
315 climatic variables as covariates:  $F_{\text{ratio}} = 1.34$ ,  $P = 0.077$ ), suggesting a strong spatial structure  
316 of the climatic component.

317

### 318 **Spatial structure of climatic factors limiting growth**

319 In the period 1951-2002, growth indices of the composite NW-C chronology were  
320 positively correlated with April temperature and May-June precipitation, whereas February-

321 March precipitation and June temperature were negatively related to growth (Fig. 4a).  
322 Composite chronologies of the NE group were also positively correlated with April  
323 temperature and May-June precipitation. Conversely, tree growth in NE sites was positively  
324 correlated with December precipitation of the previous year (Fig. 4b). The SE group  
325 chronology was positively correlated with precipitation in previous September and December,  
326 February temperature and May-June and August precipitation (Fig. 4c). Bootstrapped  
327 response functions showed that the main climatic factors limiting growth were April  
328 temperature and June temperature and precipitation in the NW-C group, December  
329 precipitation in the NE, and previous September and current May and August precipitation in  
330 SE (Fig. 4).

331

### 332 **Temporal instability of the growth-climate relationships**

333 The responses of composite group chronologies to the main limiting climatic factors were  
334 unstable during the late 20<sup>th</sup> century, reflecting a regional differentiation in the timing and  
335 duration of this non-stationary response. Radial growth in eastern groups was positively  
336 correlated with precipitation in previous December in 1947-1970 for the NE group, and since  
337 1985 for both NE and SE groups (Fig. 5a). By contrast, growth in both northern groups (NW-  
338 C and NE) showed positive relationship with April temperature since 1967, while this  
339 climatic variable was not limiting for growth in SE (Fig. 5b). All three groups showed  
340 positive relationships of growth with precipitation in May, but in particular periods for each  
341 group: 1965-1974 in NW-C, 1949-1969 in NE, and since 1994 in SE (Fig. 5c). June  
342 temperature was negatively correlated with growth in the NW-C group since 1964, and for the  
343 periods 1979-1983 for NE and 1982-1989 for SE groups. The positive response to June  
344 precipitation increased during the late decades in all groups, being significant since 1964 in  
345 NW-C, 1975 in NE and 1981 in SE (Fig. 5e).

346

347

348 **Discussion**

349

350 On a broad scale, the high correlation among site chronologies indicated a shared climatic  
351 signal in the growth patterns of Spanish *J. thurifera* populations. The geographical and  
352 climatic components explained significant fractions of the total high-frequency variation of  
353 tree growth, whereas the stand-structure component did not significantly influence growth  
354 patterns at the regional scale of study (Table 3). The degree of correlation was highly related  
355 to between-site distance, suggesting that the climatic response was spatially structured. Such  
356 spatial structure allowed us to differentiate three distinct geographical groups according to  
357 their common growth patterns in the Iberian Peninsula (NW-C, NE and SE), comprising most  
358 of the world distribution range of *J. thurifera*.

359 Elevation exerted an independent influence in structuring the between-site correlation and  
360 affected negatively the mean sensitivity of chronologies, i.e. the high-frequency variability in  
361 radial growth. The sensitivity of *J. thurifera* growth increased in the low-elevation sites (RE,  
362 SA) located in the semi-arid Middle Ebro Basin where summer droughts are more intense and  
363 frequent than in higher-elevation sites. In these semi-arid sites annual precipitation greatly  
364 fluctuates between consecutive years and likely controls tree-ring development which shows  
365 higher interannual variability. Probably, the negative relationship between elevation and mean  
366 sensitivity may be considered a characteristic of inland areas with pronounced water deficit  
367 where precipitation increases at higher elevations due to topographical effects, as occurs in  
368 other conifer forests under continental Mediterranean climates (e.g., Linares et al. 2009).  
369 Contrastingly, in wetter subalpine mountain forests, elevation and mean sensitivity are usually  
370 positively related because tree growth is mainly dependent on temperature, which is more

371 limiting for growth at higher elevation (e.g. Tardif et al. 2003; Piovesan et al. 2005; Di  
372 Filippo et al. 2007). Nevertheless, our findings need further verification since few stands  
373 appeared in mid-elevation sites (600-900 m) due to the topographical distribution of *J.*  
374 *thurifera* in the Iberian Peninsula.

375 In Mediterranean inland areas, summer drought and winter cold are the major constraints  
376 of radial growth, whereas spring is usually the most favourable season for xylem growth  
377 (Cherubini et al. 2003; Camarero et al. 2010). The secondary growth of *J. thurifera* was  
378 mostly associated to spring and early summer conditions being enhanced by warmer  
379 conditions in April and higher precipitation in May and June, in accordance with previous  
380 studies on the species (Bertaudière et al. 1999; Camarero 2006; Rozas et al. 2009). Our results  
381 are consistent with recent xylogenesis analyses in *J. thurifera*, which found that spring  
382 cambial onset, started in April or May in a warm xeric and a cold mesic site, respectively,  
383 whereas the maximum rate of wood formation was observed respectively in May or June  
384 (Camarero et al. 2010). Contrastingly, a warmer June or July, which was related to a lower  
385 growth, probably induces greater evapotranspiration, showing that water availability in late  
386 spring and early summer was crucial for growth in this species. These findings agree with the  
387 observed low growth rates in north western sites (LA and LU) and in both eastern groups,  
388 suggesting that their growing season was respectively constrained by cold spring and summer  
389 drought. These patterns indicate a strong longitudinal gradient of climate-growth relationships  
390 at broad scales, probably associated to atmospheric patterns, which is consistent with: (1) the  
391 mean size of observed regional groups of site chronologies (ca. 300 km), (2) the strong  
392 connection between geographical longitude and the second principal component of all  
393 chronologies, and (3) the geographically structured growth-climate relationships observed in  
394 the composite regional chronologies.



395 We found similarities in growth responses to climate in all composite regional  
396 chronologies, with *J. thurifera* growth being enhanced by late-winter (February) to early-  
397 spring (April) temperatures and late-Spring (May) to early-summer (June) precipitation.  
398 However, distinctive patterns were also detected which may be associated to particular  
399 climatic conditions in each region affecting carbon gain during winter. In north western and  
400 central sites growth was mainly enhanced by warm and dry conditions in late-winter and  
401 early-spring and wet summer conditions. This winter effect could be explained as the indirect  
402 influence of anticyclonic events on diurnal temperatures and the increase of solar radiation  
403 received, with the consequent rise in carbon assimilation (DeSoto 2010) and likely more  
404 intense spring growth in these cold sites (Chapin et al. 1990 and refs. therein; Larcher 2000).  
405 In high-latitude forests, this result has been interpreted as a delay in the start of the growing  
406 season due to both cold winter temperatures and high snowfall, which result in a greater depth  
407 of soil freezing and a delay of snow melt in the spring (Mäkinen et al. 2002; Euskirchen et al.  
408 2006).

409 In contrast, early winter precipitation (previous December) enhanced growth in NE and SE  
410 groups which may be caused by a greater replenishment of the soil water budget in these  
411 semi-arid areas, before tree-ring formation starts in spring when water deficit can be  
412 noticeable (Camarero et al. 2010). Furthermore, evergreen Mediterranean conifers are able to  
413 maintain the photosynthetic activity during the winter, although at lower rates than during the  
414 growing season (Larcher 2000). The surplus of carbohydrates assimilated before tree-ring  
415 formation may be stored and subsequently allocated to earlywood formation in spring after  
416 cambial reactivation (Kagawa et al. 2006). Therefore, the influence of winter precipitation on  
417 subsequent *J. thurifera* growth in all groups may be also a response to mild winter conditions  
418 leading to an increase in the assimilation of carbohydrates (Skomarkova et al. 2006; DeSoto  
419 2010), and an earlier cambial resumption. Moreover, the positive response of *J. thurifera*

420 radial growth to precipitation in the previous fall and the current spring was more important in  
421 semi-arid eastern sites (NE and SE groups) than in mesic sites westwards. Latter difference  
422 agrees with observed phenological differences between mesic and xeric sites, since spring  
423 cambial reactivation occurred *ca.* one month earlier and lasted longer under warmer (e.g. sites  
424 from the NE and SE groups) than under colder conditions (e.g. sites from the NW-C group)  
425 (Camarero et al. 2010).

426 This geographically structured climatic response of *J. thurifera* was also verified by the  
427 spatial field correlations with climatic data (see Appendix B in supplementary material).  
428 North western sites (NW-C group) were under the influence of Atlantic atmospheric patterns  
429 controlling spring precipitation and temperature at broad spatial scales. However, the positive  
430 effect of previous winter and spring precipitation on growth of eastern sites (NE and SE  
431 groups) suggested a more localised influence of cyclonic activity from the Mediterranean Sea  
432 in the eastern sites. These results confirm that the effects of atmospheric circulation patterns  
433 on *J. thurifera* growth in the Iberian Peninsula are an indirect expression of large-scale  
434 influences on local weather types and ultimate climatic factors such as precipitation,  
435 temperature and radiation as has been observed in *Pinus halepensis* (Pasho et al. 2011).

436 The shared positive response of growth to June precipitation detected over the whole  
437 Iberian distribution area of *J. thurifera* was not stationary and markedly increased during the  
438 late 20<sup>th</sup> century (Fig. 5). This increasing sensitivity to late-spring and early-summer  
439 precipitation coincided with a noticeable rise in the response of growth to April temperatures  
440 which we interpret as a consequence of the significant rise in spring temperatures and the  
441 decrease in precipitation observed since the 1970s over the Spanish Mediterranean region  
442 (Romero et al. 1998; Trenberth et al. 2007). Such increasing aridity and the occurrence of  
443 severe droughts have been revealed as one of the main factors constraining the recent growth  
444 of pine species in the Iberian Peninsula (Andreu et al. 2007). Nevertheless, we additionally

445 found that this trend of growth response was spatially structured. The timing in the climate  
446 response to the main controlling factor, i.e. June precipitation, changed among the regional  
447 groups, showing the NW-C populations an earlier and stronger responsiveness than the NE  
448 and SE ones. This pattern suggests that the positive effect of water availability in June was  
449 perceived earlier by populations in mesic sites from the NW-C group under more humid  
450 conditions than in the more xeric sites from NE and SE groups. Such pattern was not  
451 mediated by changes in the response to the previous-winter precipitation which remained high  
452 or increased slightly in xeric sites.

453 Two possible, but not mutually excluding, explanations can be proposed. First, drought  
454 stress might have begun to increase in NW-C sites earlier than in NE and SE sites, as the  
455 greater relative rise of summer temperatures in the NW-C sites as compared with eastern sites  
456 suggests (see Appendix C in supplementary material ; Christensen et al. 2007; Trenberth et al.  
457 2007). Second, *J. thurifera* populations established in more xeric sites might be more resilient  
458 and less sensitive to the decrease water availability in late spring associated with rising  
459 temperatures than those living in more humid sites, which is consistent with previous findings  
460 in *Pinus virginiana* (Orwig and Abrams 1997). Moreover, populations subjected to extreme  
461 climatic events or close to physiological limits, such as frequent severe droughts and thermal  
462 stress, might be better adapted to a warming climate than those in less hazardous and stressful  
463 environments, likely due to a directional selection for resistance (Kuparinen et al. 2010;  
464 Hoffmann and Sgrò 2011).

465

466

## 467 **Conclusions**

468 The responses of *J. thurifera* to climatic variability throughout most of its distribution  
469 range shows a strong spatial structure along its Iberian range, with a northwest-southeast shift

470 in limiting factors and response timings as a consequence of the noticeable gradient of  
471 increasing aridity. This spatial pattern may also determine future responses to global warming  
472 as non-stationary responses to water availability in late spring-early summer during the 20<sup>th</sup>  
473 century indicate that the sensitivity to climatic change may increase, especially in mesic  
474 populations at the northwest and central Iberian range of *J. thurifera*. This study foregrounds  
475 the need of comprising a major part of the geographical range of a species, including a  
476 diversity of physiographic and climatic conditions, to fully understand tree growth responses  
477 to limiting climatic factors.

478

479

#### 480 **Acknowledgements**

481 We are especially grateful to A. Fernández, J.C. Rubio and B. del Río, who helped in the  
482 laboratory, and A. Fernández, V. Fortea, J.M. Gil, R. Hernández, E. La Fuente, E. Mezquida,  
483 A. Parras, M.A. Ros, R. Serrano, C. Torices and R. Torices who helped in the field.  
484 Comments by two anonymous referees and the editor improved a previous version of the  
485 manuscript. We also thank to F. Campelo for his valuable comments and suggestions. Junta  
486 de Castilla y León supported this research with the projects VA069A07, VA006A10-2 and  
487 MEDIATIC (PTDC/AAC-CLI/103361/2008). L. DeSoto was supported by a Junta de Castilla  
488 y León and FCT postdoctoral fellowships. V. Rozas was supported by an INIA-Xunta de  
489 Galicia contract. J.J. Camarero thanks the support of ARAID and Globimed.

490

491

#### 492 **References**

493 Andreu L, Gutiérrez E, Macias M, Ribas M., Bosch O, Camarero JJ (2007) Climate increases  
494 regional tree-growth variability in Iberian pine forests. *Glob Change Biol* 13:1–12

- 495 Bertaudière V, Montès N, Gauquelin T, Édouard JL (1999) Dendroécologie du jénévrier  
496 thurifère (*Juniperus thurifera* L.): exemple de la thuriféraie de la montagne de Rié  
497 (Pyrénées, France). *Ann For Sci* 56:658–697
- 498 Biondi F, Waikul K (2004) DENDROCLIM2002. A C++ program for statistical calibration of  
499 climate signals in tree ring chronologies. *Comput Geosci* 30:303–311
- 500 Borcard D, Legendre P, Drapeau P (1992) Partialling out the spatial component of ecological  
501 variation. *Ecology* 73:1045–1055
- 502 Camarero JJ (2006) Dendroecología de *Juniperus thurifera* en zonas biogeográfica y  
503 climáticamente contrastadas. In: García-González MD, Alifriqui M, Broto M, García-  
504 Fayos P, García-López JM, Gauquelin T, Largier G, Herrero JM, Nibarere VM, Montés N,  
505 Olano JM, Sánchez-Palomares O, Sánchez-Peña G, Villar L (eds) *Actas del III Coloquio*  
506 *Internacional sobre Sabinares y Enebrales (Gen. Juniperus): Ecología y gestión forestal*  
507 *sostenible*. Junta de Castilla y León. Soria. ES, pp 79–87
- 508 Camarero JJ, Olano JM, Parras A (2010) Plastic bimodal xylogenesis in conifers from  
509 continental Mediterranean climates. *New Phytol* 185: 471–480
- 510 Carrer M, Nola P, Eduard JL, Motta R, Urbinati C (2007) Regional variability of climate-  
511 growth relationships in *Pinus cembra* high elevation forests in the Alps. *J Ecol*  
512 95:1072–1083
- 513 Carrer M, Nola P, Motta R, Urbinati C (2010) Contrasting tree-ring growth to climate  
514 responses of *Abies alba* toward the southern limit of its distribution area. *Oikos* 119:1515–  
515 1525
- 516 Chapin III FS, Schulze ED, Mooney HA (1990) The ecology and economics of storage in  
517 plants. *Annu Rev Ecol Syst* 21:423–447

- 518 Cherubini P, Gartner BL, Tognetti R, Bräker OU, Schoch W, Innes JL (2003) Identification,  
519 measurement and interpretation of tree rings in woody species from Mediterranean  
520 climates. *Biol Rev* 78:119–148
- 521 Christensen JH, Hewitson B, Busuioc A, Chen A, Gao X, Held I, Jones R, Kolli RK, Kwon  
522 W-T, Laprise R, Magaña Rueda V, Mearns L, Menéndez CG, Räisänen J, Rinke A, Sarr A,  
523 Whetton P (2007) Regional Climate Projections. In: Solomon S, Qin D, Manning M, Chen  
524 Z, Marquis M, Averyt KB, Tignor M, Miller HL (eds) *Climate Change 2007: The Physical  
525 Science Basis. Contribution of Working Group I to the Fourth Assessment Report of the  
526 Intergovernmental Panel on Climate Change*. Cambridge University Press, Cambridge,  
527 United Kingdom and New York, NY, USA, pp 847–940
- 528 Cook ER, Holmes RL (1996) Guide for computer program ARSTAN. In: Grissino-Mayer  
529 HD, Holmes RL, Fritts, HC (eds) *The International Tree-Ring Data Bank Program Library  
530 Version 2.0 User's Manual*. Laboratory of Tree-Ring Research, University of Arizona,  
531 Tucson, USA, pp 75–87
- 532 Cook ER, Glitzenstein JS, Krusic PJ, Harcombe PA (2001) Identifying functional groups of  
533 trees in West Gulf Coast forests (USA): a tree-ring approach. *Ecol Appl* 11:883–903
- 534 Cook ER, Kairiukstis L (1990) *Methods of Dendrochronology: Applications in the  
535 Environmental Sciences*. Kluwer Academic Publishers, Dordrecht, The Netherlands
- 536 Cook ER, Peters K (1981) The smoothing spline: a new approach to standardizing forest  
537 interior tree-ring width series for dendroclimatic studies. *Tree-Ring Bull* 4:45–53
- 538 CRU (2008) University of East Anglia Climate Research Unit (CRU). CRU Datasets,  
539 [Internet]. British Atmospheric Data Centre, 2008, 29 December 2009. Available from  
540 <http://badc.nerc.ac.uk/data/cru>
- 541 Davis MB, Shaw RG (2001) Range shifts and adaptive responses to quaternary climate  
542 change. *Science* 292:673–679

- 543 De Martonne E (1925) *Traité de Géographie Physique*. Colin, Paris, France
- 544 DeSoto L (2010) Global change effect on the dioecious tree *Juniperus thurifera* in the Iberian  
545 Peninsula. Dissertation, University of Valladolid, Soria, Spain
- 546 Desper R, Gascuel O (2002) Fast and accurate phylogeny reconstruction algorithms based on  
547 the minimum-evolution principle. *J Comput Biol* 9:687–705
- 548 Di Filippo A, Biondi F, Cufar K, de Luis M, Gragner M, Maugeri M, Presutti E, Schirone B,  
549 Piovesan G (2007) Bioclimatology of beech (*Fagus sylvatica* L.) in the Eastern Alps:  
550 spatial and altitudinal climatic signals identified through a tree-ring network. *J Biogeogr*  
551 34:1873–1892
- 552 Esteban-Parra MJ, Rodrigo FS, Castro-Diez Y (1998) Spatial and temporal patterns of  
553 precipitation in Spain for the period 1880-1992. *Int J Climatol* 18:1557–1574
- 554 Euskirchen ES, McGuire AD, Kicklighter DW, Zhuang Q, Clein JS, Dargaville RJ, Dye DG,  
555 Kimball HS, McDonald KC, Melillo JM, Romanovsky VE, Smith NV (2006) Importance  
556 of recent shifts in soil thermal dynamics on growing season length, productivity, and  
557 carbon sequestration in terrestrial high-latitude ecosystems. *Glob Change Biol* 12:731–750
- 558 Fritts HC (1976) *Tree Rings and Climate*. Academic Press, London, UK
- 559 Fritts HC, Vaganov EA, Sviderskaya IV, Shashkin AV (1991) Climatic variation and tree-  
560 ring structure in conifers: empirical and mechanistic models of tree-ring width, number of  
561 cells, cell-size, cell-wall thickness and wood density. *Clim Res* 1:97–116
- 562 Garfin GM (1998) Relationships between winter atmospheric circulation patterns and extreme  
563 tree growth anomalies in the Sierra Nevada. *Int J Climatol* 18:725–740
- 564 Gaston KJ (2009) Geographic range limits: achieving synthesis. *Proc R Soc B*  
565 276:1395–1406

- 566 Gauquelin T, Bertaudiere V, Montes N, Badri W, Asmode JF (1999) Endangered stands of  
567 thuriferous juniper in the western Mediterranean basin: ecological status, conservation and  
568 management. *Biodiv Conserv* 8:1479–1498
- 569 Gorczynski L (1922) The calculation of the degree of continentality. *Mon Weather Rev*  
570 50:370–370
- 571 Grissino-Mayer HD (2001) Evaluating crossdating accuracy: A manual and tutorial for the  
572 computer program COFECHA. *Tree-Ring Res* 57:205–221.
- 573 Hoffmann AA, Sgrò CM (2011) Climate change and evolutionary adaptation. *Nature*  
574 470:479–485.
- 575 Holmes RL (1983) Computer-assisted quality control in tree-ring dating and measurement.  
576 *Tree-Ring Bull* 43:69–78
- 577 Holmes RL (1994) *Dendrochronology Program Library Users Manual*. Laboratory of Tree-  
578 Ring Research, University of Arizona, Tucson. USA
- 579 Jiménez JF, Werner O, Sánchez-Gómez P, Fernández S, Guerra J (2003) Genetic variations  
580 and migration pathways of *Juniperus thurifera* L. (Cupressaceae) in the western  
581 Mediterranean region. *Isr J Plant Sci* 51:1–22
- 582 Jump AS, Hunt JM, Peñuelas J (2006) Rapid climate change related growth decline at the  
583 southern range-edge of *Fagus sylvatica*. *Glob Change Biol* 12:2163–2174
- 584 Kagawa A, Sugimoto A, Maximov TC (2006)  $^{13}\text{C}$  pulse-labelling of photoassimilates  
585 reveals carbon allocation within and between tree rings. *Plant Cell Environ* 29:1571–1584
- 586 Kupařinen A, Savolainen O, Schurr FM (2010) Increased mortality can promote evolutionary  
587 adaptation of forest trees to climate change. *For Ecol Manage* 259:1003–1008
- 588 Larcher, W. (2000) Temperature stress and survival ability of Mediterranean sclerophyllous  
589 plants. *Plant Biosyst.* 134, 279–295
- 590 Legendre P, Legendre L (1998) *Numerical Ecology*. Elsevier, Amsterdam. The Netherlands



- 591 Leonelli G, Pelfini M, Battipaglia G, Cherubini P (2009) Site-aspect influence on climate  
592 sensitivity over time of a high-altitude *Pinus cembra* tree-ring network. *Clim Change*  
593 96:185–201
- 594 Linares JC, Camarero JJ, Carreira JA (2009) Interacting effects of climate and forest-cover  
595 changes on mortality and growth of the southernmost European fir forests. *Glob Ecol*  
596 *Biogeogr* 18:485–497
- 597 Loehle C, LeBlanc D (1996) Model-based assessments of climate change effects on forests: a  
598 critical review. *Ecol Model* 90:1–31
- 599 Macias M, Andreu L, Bosch O, Camarero JJ, Gutiérrez E (2006) Increasing aridity is  
600 enhancing silver fir (*Abies alba* Mill.) water stress in its southwestern distribution limit.  
601 *Clim Change* 79:289–313
- 602 Mäkinen H, Nöjd P, Kahle H-P, Neumann U, Tveite B, Mielikäinen K, Röhle H, Spiecker H  
603 (2002) Radial growth variation of Norway spruce (*Picea abies* (L.) Karst.) across  
604 latitudinal and altitudinal gradients in central and northern Europe. *For Ecol Manage*  
605 174:233–249
- 606 Mitchell TD, Jones PD (2005) An improved method of constructing a database of monthly  
607 climate observations and associated high-resolution grids. *Int J Climatol* 25:693–712
- 608 Mitrakos KA (1980) A theory for Mediterranean plant life. *Acta Oecol* 1:245–252
- 609 Orwig DA, Abrams MD (1997) Variation in radial growth responses to drought among  
610 species, site, and canopy strata. *Trees-Struct Funct* 11:474–484
- 611 Paradis E, Claude J, Strimmer K (2004) APE: analyses of phylogenetics and evolution in R  
612 language. *Bioinformatics* 20:289–290.
- 613 Pasho E, Camarero JJ, de Luis M, Vicente-Serrano SM (2011) Spatial variability in large-  
614 scale and regional atmospheric drivers of *Pinus halepensis* growth in eastern Spain. *Agr*  
615 *For Meteo* 151:1106–1119

- 616 Piovesan G, Biondi F, Bernabei M, Di Filippo A, Schirone B (2005) Spatial and altitudinal  
617 bioclimatic zones of the Italian peninsula identified from a beech (*Fagus sylvatica* L.) tree-  
618 ring network. *Acta Oecol* 27:197–210
- 619 R Development Core Team (2010) R: A Language and Environment for Statistical  
620 Computing. R Foundation for Statistical Computing, Vienna. Austria
- 621 Rivas-Martínez S, Rivas-Sáenz S (2009) Sistema de Clasificación Bioclimática Mundial,  
622 1996–2009. Centro de Investigaciones Fitosociológicas, Madrid.  
623 <http://www.ucm.es/info/cif>
- 624 Rodríguez-Puebla C, Encinas AH, Nieto S, Garmendia J (1998) Spatial and temporal patterns  
625 of annual precipitation variability over the Iberian Peninsula. *Int J Clim* 18:299–316
- 626 Romero R, Guijarro JA, Ramis C, Alonso S (1998) A 30-year (1964–1993) daily rainfall data  
627 base for the Spanish Mediterranean regions: first exploratory study. *Int J Clim* 18:541–560
- 628 Rozas V, DeSoto L, Olano JM (2009) Sex-specific, age-dependent sensitivity of tree-ring  
629 growth to climate in the dioecious tree *Juniperus thurifera*. *New Phytol* 182:687–697
- 630 Sarris D, Christodoulakis D, Körner C (2007) Recent decline in precipitation and tree growth  
631 in the eastern Mediterranean. *Glob Change Biol* 13:1187–1200
- 632 Stokes MA, Smiley TL (1996) An Introduction to Tree-Ring Dating. The University of  
633 Arizona Press, Tucson. USA
- 634 Svenning J-C, Skov F (2004) Limited filling of the potential range in European tree species.  
635 *Ecol Lett* 7:565–573
- 636 Skomarkova MV, Vaganov EA, Mund M, Knohl A, Linke P, Boerner A, Schulze E.-D.  
637 (2006) Inter-annual and seasonal variability of radial growth, wood density and carbon  
638 isotope ratios in tree rings of beech (*Fagus sylvatica*) growing in Germany and Italy.  
639 *Trees-Struct Funct* 20:571–586

- 640 Tardif J, Camarero JJ, Ribas M, Gutiérrez E (2003) Spatiotemporal variability in tree growth  
641 in the central Pyrenees: climatic and site influences. *Ecol Monogr* 73:241–257
- 642 ter Braak CJF (1986) Canonical correspondence analysis, a new eigenvector technique for  
643 multivariate direct gradient analysis. *Ecology* 67:1167–1179
- 644 ter Braak CJF (1988) CANOCO – A FORTRAN program for canonical community  
645 ordination by [partial] [detrended] [canonical] correspondence analysis, principal  
646 components analysis and redundancy analysis (version 2.1). Agricultural Mathematics  
647 Group, Wageningen. The Netherlands
- 648 ter Braak CJF, Šmilauer P (1997) Canoco for Windows Version 4.0. Centre for Biometry.  
649 Wageningen. The Netherlands
- 650 Thuiller W, Albert CH, Araújo MB, Berry PM, Cabeza M, Guisan G, Hickler T, Midgley GF,  
651 Paterson J, Schurr FM, Sykes MT, Zimmermann NE (2008) Predicting global change  
652 impacts on plant species distributions: future challenges. *Perspect Plant Ecol Evol Syst*  
653 9:137–152
- 654 Trenberth KE, Jones PD, Ambenje P, Bojariu R, Easterling D, Klein Tank A, Parker D,  
655 Rahimzadeh F, Renwick JA, Rusticucci M, Soden B, Zhai P (2007) Observations: Surface  
656 and Atmospheric Climate Change. In: Solomon S, Qin D, Manning M, Chen Z, Marquis  
657 M, Averyt KB, Tignor M, Miller HL (eds) *Climate Change 2007: The Physical Science*  
658 *Basis. Contribution of Working Group I to the Fourth Assessment Report of the*  
659 *Intergovernmental Panel on Climate Change. Cambridge University Press, Cambridge,*  
660 *United Kingdom and New York, NY, USA, pp. 235–336*
- 661 van Oldenborgh GJ, Drijfhout S, van Ulden A, Haarsma R, Sterl A, Severijns C, Hazeleger  
662 W, Dijkstra H (2008) Western Europe is warming much faster than expected. *Clim Past*  
663 5:1–12

664 **Table 1.** Geographical and structural features of the thirteen study sites. Site name, code,  
 665 geographical latitude and longitude, elevation, mean (range) values for tree age, diameter at  
 666 breast height (DBH) and height are displayed. Sites' locations are displayed in Figure 1a.

667

Group	Site	Code	Latitude (N)	Longitude (W)	Elevation (m a.s.l.)	Age (years)*	DBH (cm)	Height (m)
NW-C	Arlanza	AR	42° 02' 49"	3° 26' 42"	932	72 (57-87)	24.8 (18.5-30.1)	8.0 (6.1-12.2)
	Sigueruelo	SI	41° 10' 04"	3° 38' 15"	1114	206 (102-413)	60.9 (33.4-85.3)	8.3 (6.0-12.0)
	Cabrejas del Pinar	CA	41° 47' 37"	2° 50' 42"	1130	132 (87-209)	20.2 (12.8-35.1)	6.5 (4.2-10.8)
	Peña Lampa	LA	42° 50' 31"	4° 51' 36"	1187	97 (77-125)	20.1 (12.4-31.7)	6.0 (4.1-9.2)
	Mirantes de Luna	LU	42° 52' 39"	5° 51' 05"	1284	103 (60-136)	13.9 (9.1-22)	5.0 (3.3-8.2)
	Buenache de la Sierra	BU	40° 07' 46"	1° 58' 26"	1319	85 (46-115)	29.5 (21.3-37.6)	8.2 (5.7-10.8)
NE	Retuerta de Pina	RE	41° 28' 00"	0° 16' 31"	358	50 (32-63)	22.4 (5.6-35.5)	7.1 (4.5-10.0)
	Santa Engracia	SA	41° 46' 35"	0° 32' 29"	530	73 (40-136)	19.6 (12.9-24.8)	5.6 (4.5-6.2)
	Ciria	CI	41° 37' 43"	1° 56' 17"	1157	91 (66-114)	32.3 (21.6-41.8)	7.9 (4.7-10.8)
	Chaorna	CH	41° 07' 45"	2° 11' 21"	1210	93 (48-137)	37.4 (20.0-72.0)	6.9 (4.0-8.9)
SE	Viveros	VI	38° 47' 55"	2° 31' 34"	1030	83 (56-115)	25.9 (19.1-31.8)	5.9 (4.9-7.8)
	Veguillas de la Sierra	VE	40° 09' 26"	1° 25' 51"	1375	154 (61-199)	38.8 (25.0-56.5)	5.7 (4.0-8.0)
	Olmedilla	OL	40° 19' 12"	0° 44' 01"	1400	75 (58-98)	28.5 (19.0-42.5)	7.4 (6.1-9.9)

668 \*Age was estimated as the maximum number of rings counted at 1.3 m.

669 **Table 2.** Summary of the dendrochronological statistics calculated for the ring-width  
 670 chronologies of each site for the common period 1951-2002. Sites' codes are as in Table 1.  
 671

Group	Site	Period	No. trees/radii	Raw tree-ring data		Residual chronology				
				MW $\pm$ SD (mm)	AC	ms <sub>x</sub>	r <sub>bt</sub>	EPS	E1 (%)	SNR
NW-C	AR	1925-2007	14 / 26	1.21 $\pm$ 0.59	0.67	0.16	0.41	0.86	45.40	9.40
	SI	1894-2006	11 / 21	1.09 $\pm$ 0.43	0.67	0.32	0.39	0.88	43.94	7.03
	CA	1850-2004	23 / 31	1.13 $\pm$ 0.41	0.72	0.21	0.37	0.93	42.44	13.48
	LA	1902-2006	14 / 21	0.70 $\pm$ 0.32	0.69	0.22	0.45	0.86	46.89	6.35
	LU	1876-2002	18 / 29	0.56 $\pm$ 0.20	0.80	0.30	0.47	0.93	48.43	13.46
	BU	1920-2006	15 / 22	1.24 $\pm$ 0.48	0.67	0.19	0.39	0.91	43.94	9.72
NE	RE	1945-2005	12 / 20	0.93 $\pm$ 0.52	0.54	0.31	0.54	0.94	58.80	14.36
	SA	1924-2006	13 / 28	0.96 $\pm$ 0.58	0.42	0.45	0.37	0.85	44.50	5.73
	CI	1911-2006	14 / 24	1.17 $\pm$ 0.54	0.63	0.31	0.38	0.90	43.12	8.61
	CH	1920-2006	13 / 22	1.13 $\pm$ 0.40	0.59	0.16	0.38	0.84	43.60	7.14
SE	VI	1922-2006	13 / 19	1.27 $\pm$ 0.57	0.57	0.33	0.38	0.85	43.47	5.10
	VE	1840-2006	19 / 31	0.62 $\pm$ 0.25	0.72	0.17	0.41	0.89	34.50	8.41
	OL	1909-2005	12 / 21	0.86 $\pm$ 0.38	0.65	0.24	0.42	0.90	46.51	8.71

672  
 673 MW, mean ring-width; SD, ring-width standard deviation; AC, first-order autocorrelation;  
 674 ms<sub>x</sub>, mean sensitivity; r<sub>bt</sub>, mean between-trees correlation; EPS, expressed population signal;  
 675 E1, variance explained by the first principal component; SNR, signal-to-noise ratio.

676 **Table 3.** Variables included in the RDA models of tree growth for the period 1951-2002 after  
 677 a stepwise forward procedure. The  $F$ -ratio statistic and the probability level ( $P$ ) are also  
 678 displayed. The significance level of the model was based on 999 randomizations. Only those  
 679 environmental variables with significant effects ( $P < 0.05$ ) on tree-ring growth, according to a  
 680 stepwise selection procedure, are included. Reduced models included all environmental  
 681 variables with significant effects on tree growth variability.

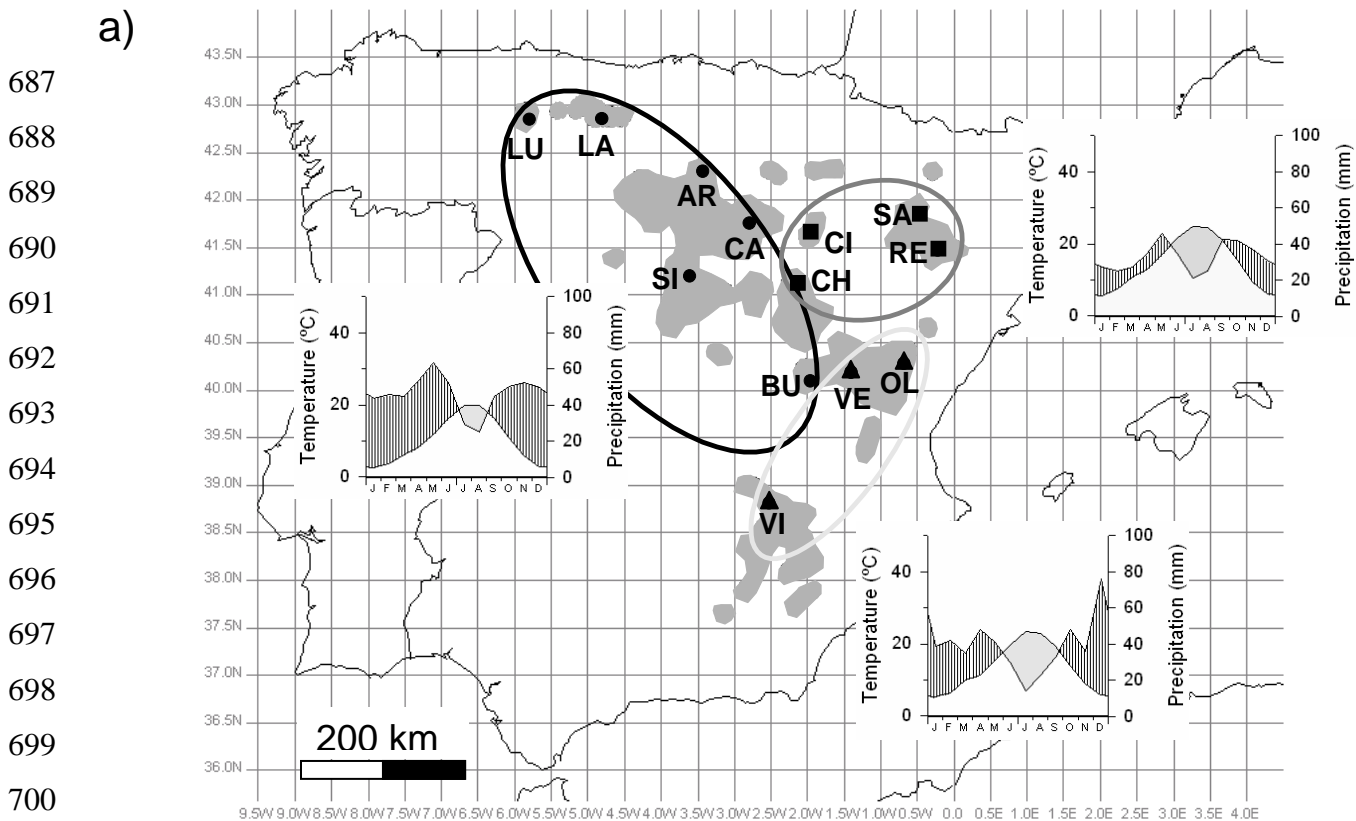
682

Reduced model	$F$ -ratio	$P$	Variables	$\lambda^a$	$F$ -ratio	$P$
Geographical variables	2.20	< 0.001	Elevation	0.19	2.50	0.004
			Latitude	0.11	1.72	0.030
Climatic variables	2.32	< 0.001	Mean temperature	0.16	2.25	0.010
			Mediterraneity index	0.15	2.16	0.009

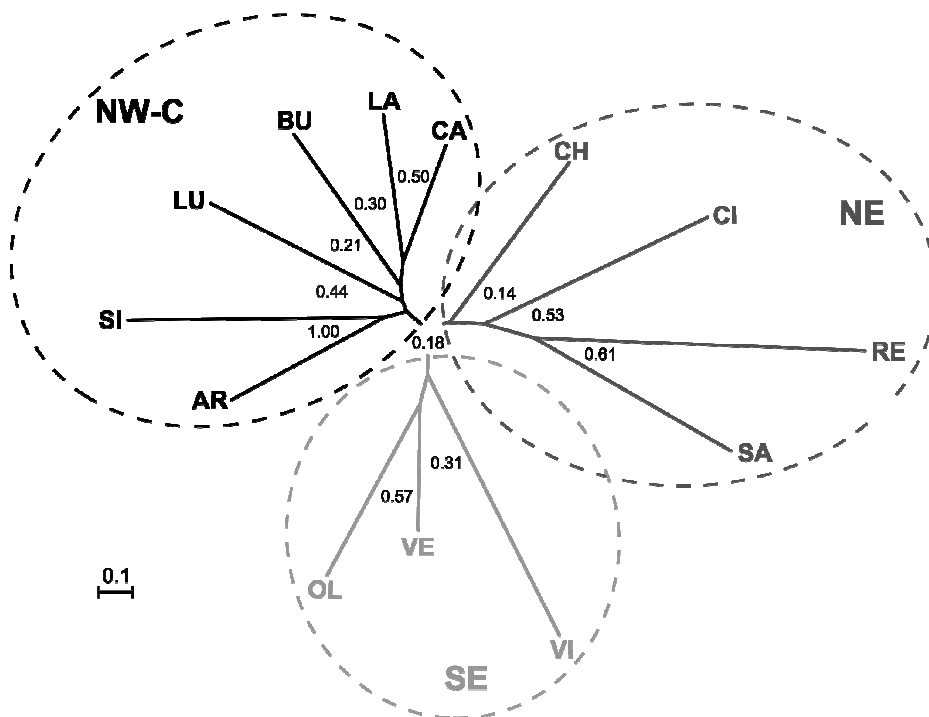
683 <sup>a</sup>  $\lambda$ : eigenvalues for the corresponding extracted axes, equivalent to the proportion of site  
 684 growth variance explained by each environmental variable.

685 Figures

686 **Figure 1**



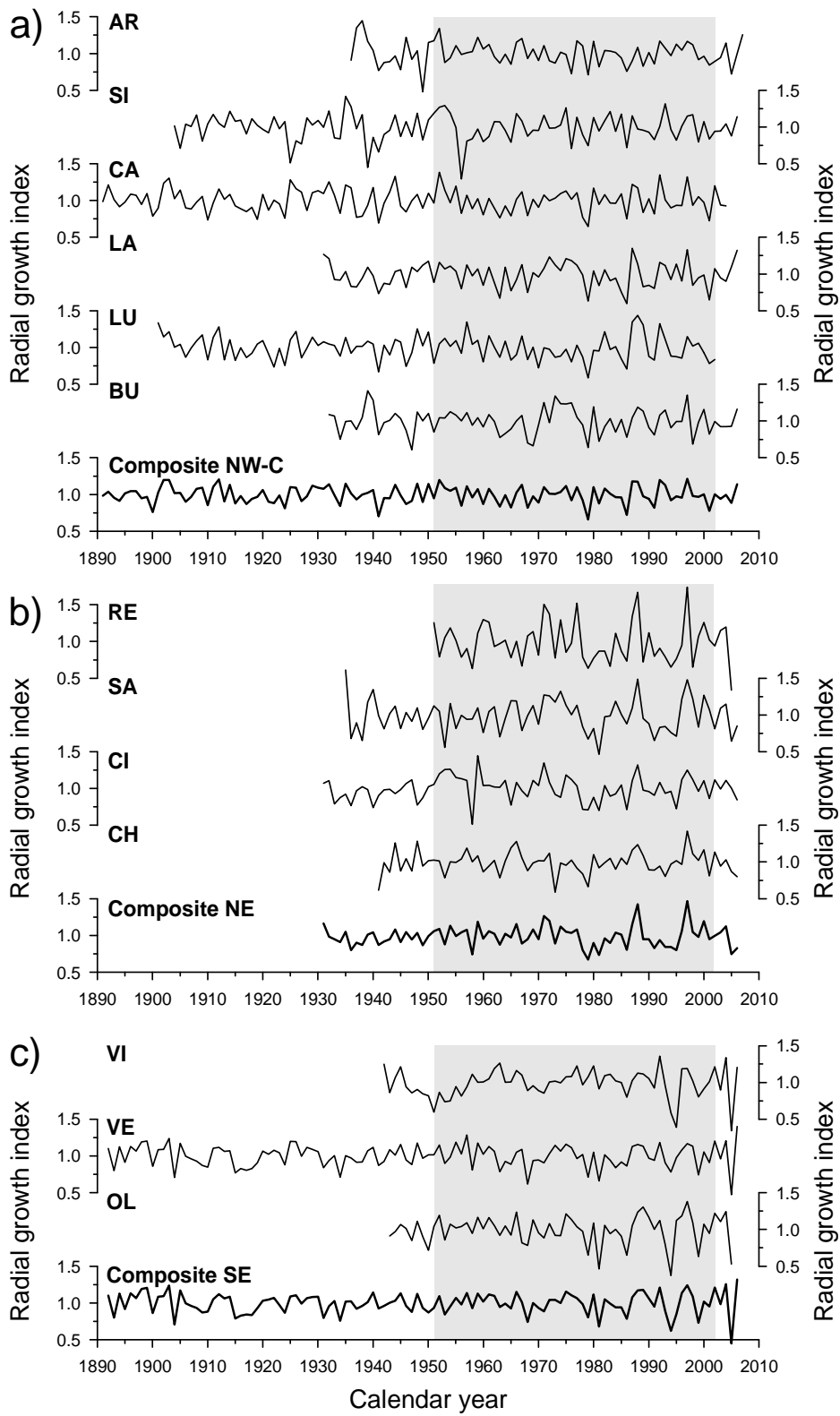
b)



701

702 **Figure 2**

703

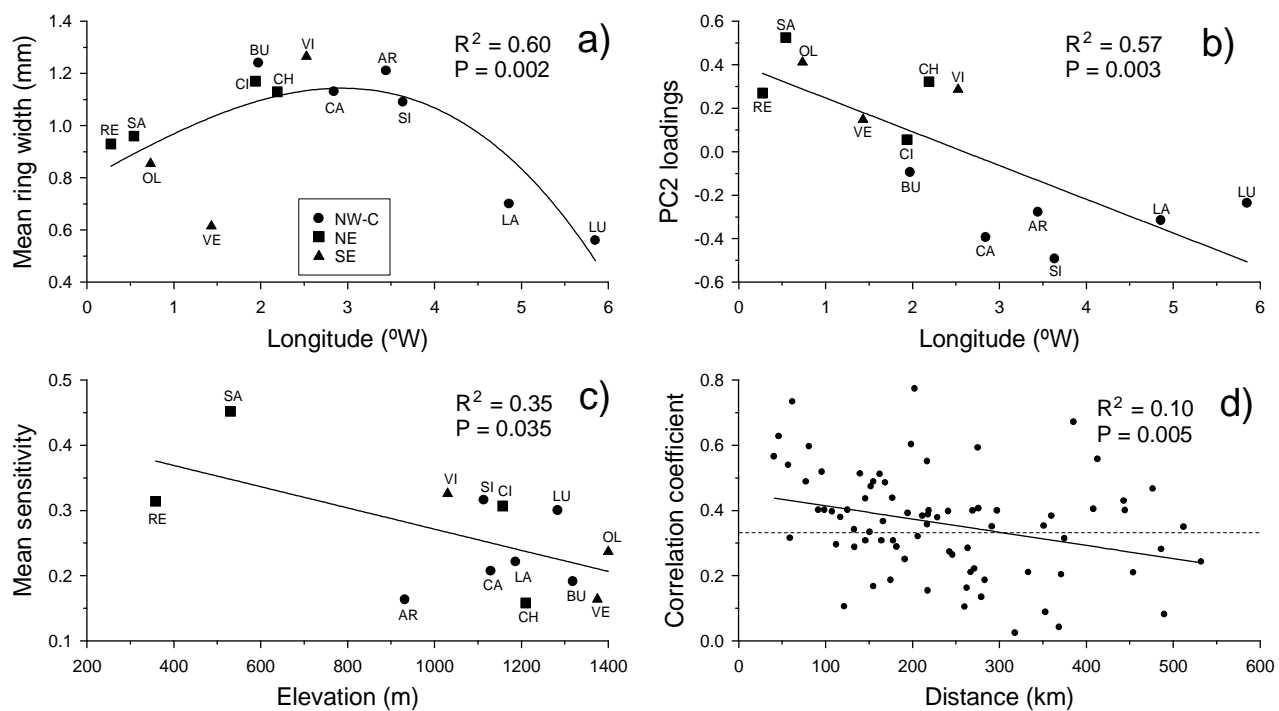


704



705 **Figure 3**

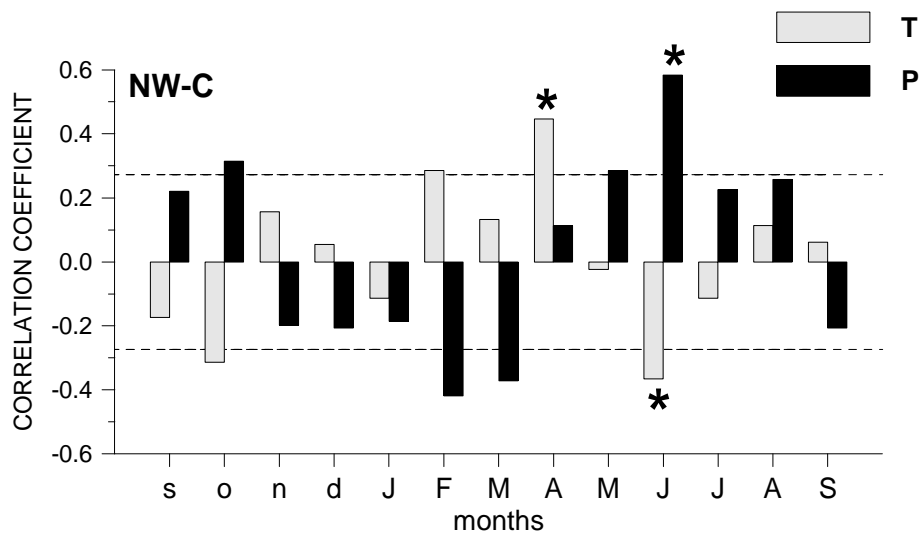
706



707

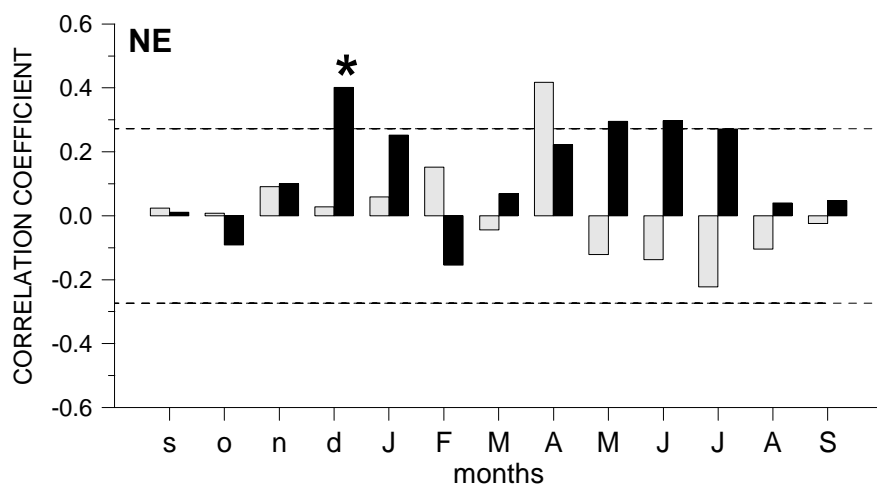
708 **Figure 4**

a)



709

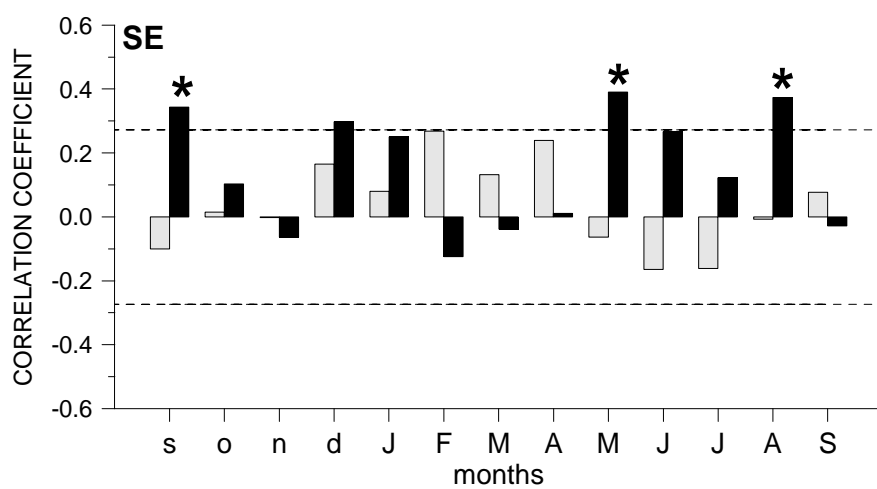
b)



710

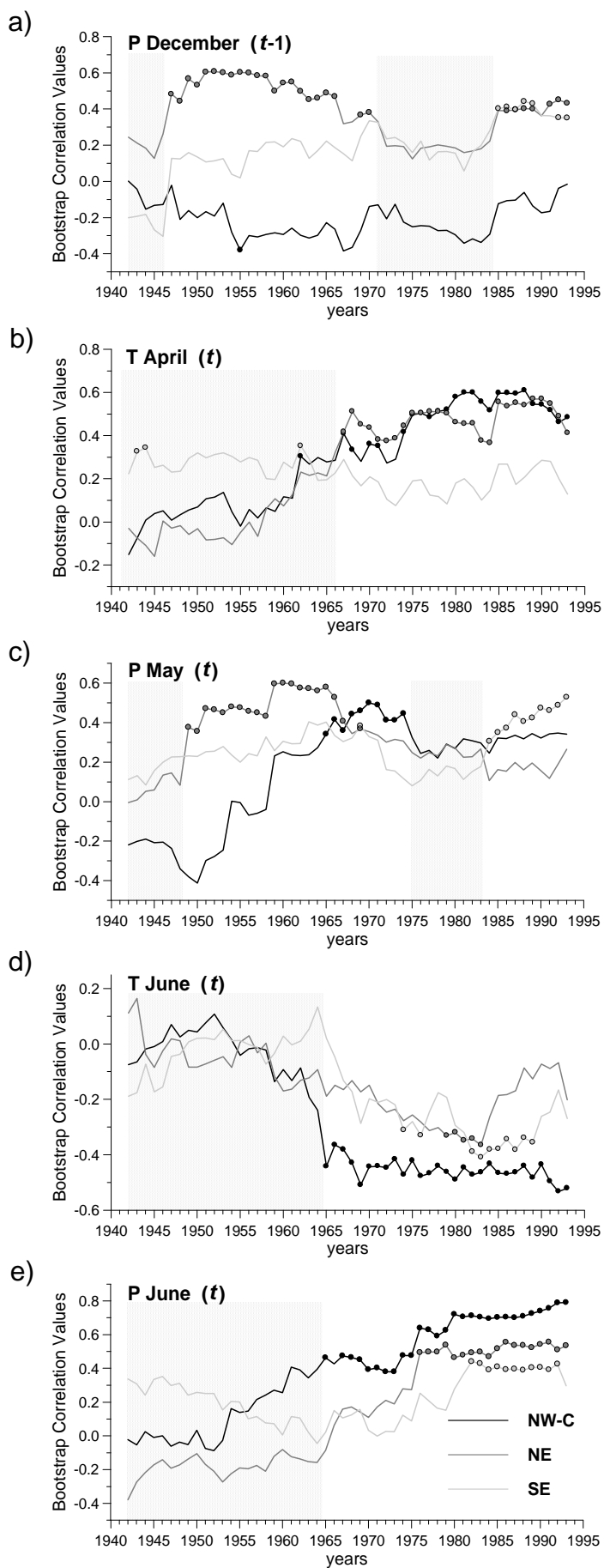
711

c)



712

713 **Figure 5**



714 **Figure legends**

715

716 **Figure 1.** (a) Sampled *Juniperus thurifera* stands within the species distribution area in Spain  
717 (grey areas) and corresponding regional groups detected using hierarchical cluster analysis for  
718 the period 1951-2002: North West and Centre (NW-C), North East (NE) and South East (SE).  
719 Climate diagrams of representative climatic stations for each group are displayed (NW-C,  
720 Soria, 41° 46' N, 2° 28' W, 1063 m a.s.l.; NE, Pallaruelo de Monegros, 41° 42' N, 0° 12' W,  
721 356 m; SE; Nerpio, 38° 09' N, 02° 18' W, 1082 m). (b) Regional groups recognised using  
722 hierarchical cluster analysis for the period 1951-2002. NW-C in black, NE sites in dark grey,  
723 and SE in light grey. The values on nodes are the proportion of bootstrapped clusters that  
724 support the groupings showed in HCA analysis. Sites' codes are indicated in Table 1.

725

726 **Figure 2.** Residual ring-width chronologies of the thirteen *J. thurifera* study sites belonging  
727 to NW-C (a), NE (b) and SE (c) groups. The site chronologies and the composite regional  
728 chronologies of each group are shown. The common period 1951-2002 is shaded.

729

730 **Figure 3.** Relationships of (a) mean tree-ring width and (b) second principal component  
731 (PC2) loadings for the site chronologies vs. geographical longitude, (c) mean sensitivity of the  
732 site chronologies vs. elevation, and (d) correlation coefficient between site chronologies vs.  
733 inter-site distance (teleconnection pattern). Solid lines represent quadratic (a) or linear (b, c,  
734 d) regressions with their corresponding  $R^2$  and  $P$  values. Different symbols correspond to  
735 different regional groups (NW-C, North West and Centre; NE, North East; SE, South East).  
736 The dotted line in Figure 3d indicates the significance level ( $P < 0.05$ ) for correlation  
737 coefficients.

738

739 **Figure 4.** Correlation coefficients calculated between radial growth and climate for the period  
740 1951-2002 among the ring-width indices of the regional composite chronologies (a, NW-C; b,  
741 NE; c, SE) and gridded monthly climatic data (T, mean temperature, and P, total  
742 precipitation), over a 13-month window. Months before (year  $t-1$ ) and during tree-ring  
743 formation (year  $t$ ) are abbreviated by lower- and upper-case letters, respectively. Black lines  
744 indicate the 95% significance level for the Pearson correlation coefficients, and asterisks  
745 indicate significant ( $P < 0.05$ ) response function coefficients.

746

747 **Figure 5.** Temporal shifts of correlations between *J. thurifera* regional composite  
748 chronologies (NW-C, North West-Central; NE, North East; SE, South East) and selected  
749 monthly precipitation (P) and mean temperature (T) data of the previous ( $t-1$ ) and current ( $t$ )  
750 years: previous December P (a); current April T (b); current May P (c); current June T (d),  
751 current June P (e). Moving bootstrap correlations were calculated for 25-year intervals in the  
752 period 1930-2006, and each correlation corresponds to the middle of the interval. Significant  
753 correlations are displayed as circles ( $P < 0.05$ ). The grey background highlights the periods  
754 with non-significant correlations in at least five consecutive intervals.